ON THE EFFECTS OF WAVE AMPLITUDE, DAMPING AND INITIAL CONDITIONS ON THE PARAMETRIC ROLL RESONANCE

Jerzy Matusiak, Helsinki University of Technology, Ship Laboratory (Finland)

Abstract

Parametric resonance of roll is simulated numerically. Simulated cases correspond to the model tests conducted with a free running model of a modern fast RoPax vessel. Tests were conducted for a number of ship speed values in the head and in the following regular waves. Simulation is conducted using the so-called two-stage approach of evaluating the dynamic ship motions in the six-degrees-of-freedom.

Generally, a good agreement between the simulation and the test results is noted. The simulations reveal a resonant roll motion for the condtions of it's occurence as observed in the model tests. The effect of wave amplitude and the effect of roll damping on the time required for the resonant motion to start is well reproduced by the simulations. The effect of the initial heel on this required time is also discussed with an aid of simulations.

1 INTRODUCTION

An extensive model test series of a modern, fast twin-screw Ro-Pax vessel was conducted at the Ship Laboratory of the Helsinki University of Technology. Tests were primarily concerned with the dynamic stability. In particular, a loss of stability on a crest of a following wave and parametric roll resonance were investigated both in regular and irregular waves for three KG-values with ship model without and with two different height bilge keels (450 mm and 900 mm in the full scale). Tests were run with the self-propelled model steered manually [4]. Main particulars of the vessel are given in Table below.

Table: Main particulars of the vessel.

	Full scale	Model
Scale	1	39.024
L_{wl} [m]	158.6	4.064
L_{pp} [m]	158	4.049
D_p [m]	4.8	0.123
B [m]	25	0.641
B_{wl} [m]	25	0.641
T_a [m]	6.1	0.156
T_f [m]	6.1	0.156
D [m]	15	0.384
∇ [m^3]	13766	0.232
M_m [kg]		231.40
S [m^2]	4356	2.860
C_B	0.571	0.571
L_{wl}/B_{wl}	6.344	6.344
B_{wl}/T_{wl}	4.098	4.098
$L_{wl}/\nabla^{(1/3)}$	6.618	6.618

	Full scale	Model
KG [m]	11, 11.5, 12	0.282, 0.295, 0.307

Stabilty lever curve of the vessel is shown in Fig. 1

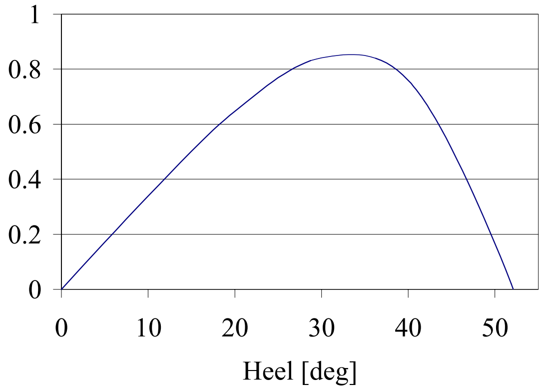

Fig. 1 Static stability lever curve of the investigated vessel for the height of the centre of gravity KG = 12 [m].

2 THE METHOD USED IN THE NUMERICAL SIMULATION

Numerical simulation of the selected test runs in regular head waves were conducted using the so-called two-stage approach of ship dynamic response evaluation [5, 6]. This is a general model of ship dynamics incorporating the non-linear sea-keeping in the six-degrees-of-freedom and the elements of maneouvring. The same method was used, amongst the others, in the benchmark study of the 23rd ITTC dedicated to the dynamic stability of two ships. The main goal of the presented study was to validate the two-stage approach using the model test experiments dedicated to the parametric roll resonance of a modern Ro-Pax vessel.

The basic idea behind the two-stage approach can be explained with an aid of a simple non-linear Single-Degree-Of-Freedom (SDOF) system given by the equation

$$m\ddot{X} + g(\dot{X}) + h(X) = F(X;t)\,, \tag{1}$$

where m is system mass, t is time. Dots denote time derivatives. The functions g and h are in general non-linear functions of response velocity $\dot{X}$ and displacement X, respectively. Function F is also a non-linear function of X describing the external excitation to the system. The linear version of the equation (1) is given by

$$m\ddot{x}_L + c\dot{x}_L + kx_L = F_L(t)\,, \tag{2}$$

where F_L is a linear, independent of the response forcing function. The total response is decomposed into a linear part x_L and a non-linear portion x as

$$X = x_L + x. \tag{3}$$

Subtracting linear approximation (2) from the general equation (1) yields an equation for the non-linear part x of the response

$$m\ddot{x} + \left[g(\dot{x}_L + \dot{x}) - c\dot{x}_L\right] + \left[h(x_L + x) - kx_L\right] = f \tag{4}$$

where $f = F(X;t) - F_L(t)$ is a non-linear part of the forcing function.

In the two-stage approach applied to the ship motion dynamics the total response and loading are decomposed into the linear approximation (denoted by subscript L) and the non-linear portion (responses: u,v,w,P,Q,R and loading: X,Y,Z,K,M,N). Linear approximation of the responses is evaluated using the transfer functions yielded by the linear strip theory [3] and using an information of the instanteneous ship position in respect to the wave. The following lengthy set of equations of the non-linear part of motion (see reference [5] for the details of derivation) is obtained:

$$
\begin{aligned}
&\mathrm{m}\left[\dot{u}+(Q_{\mathrm{L}}+Q)(w_{\mathrm{L}}+w)-(R_{\mathrm{L}}+R)(v_{\mathrm{L}}+v)\right.\\
&\left.+g\sin(\theta_{\mathrm{L}}+\theta)\right]=X\\
&\mathrm{m}\left[\dot{v}+(R_{\mathrm{L}}+R)u-(P_{\mathrm{L}}+P)(w_{\mathrm{L}}+w)\right.\\
&\left.-g\cos(\theta_{\mathrm{L}}+\theta)\sin(\phi_{\mathrm{L}}+\phi)\right]=Y\\
&\mathrm{m}\left[\dot{w}+(P_{\mathrm{L}}+P)(v_{\mathrm{L}}+v)-(Q_{\mathrm{L}}+Q)u\right.\\
&\left.-g\cos(\theta_{\mathrm{L}}+\theta)\cos(\phi_{\mathrm{L}}+\phi)\right]=Z\\
&\left[I_z(R_{\mathrm{L}}+R)-I_{zx}(P_{\mathrm{L}}+P)-I_{zy}(Q_{\mathrm{L}}+Q)\right](Q_{\mathrm{L}}+Q)\\
&-\left[I_y(Q_{\mathrm{L}}+Q)-I_{yz}(R_{\mathrm{L}}+R)-I_{yx}(P_{\mathrm{L}}+P)\right](R_{\mathrm{L}}+R)\\
&+I_x\dot{P}-I_{xy}\dot{Q}-I_{xz}\dot{R}=K\\
&\left[I_x(P_{\mathrm{L}}+P)-I_{xy}(Q_{\mathrm{L}}+Q)-I_{xz}(R_{\mathrm{L}}+R)\right](R_{\mathrm{L}}+R)\\
&-\left[I_z(R_{\mathrm{L}}+R)-I_{zx}(P_{\mathrm{L}}+P)-I_{zy}(Q_{\mathrm{L}}+Q)\right](P_{\mathrm{L}}+P)\\
&+I_y\dot{Q}-I_{yx}\dot{P}-I_{yz}\dot{R}=M\\
&\left[I_y(Q_{\mathrm{L}}+Q)-I_{yz}(R_{\mathrm{L}}+R)-I_{yx}(P_{\mathrm{L}}+P)\right](P_{\mathrm{L}}+P)\\
&-\left[I_x(P_{\mathrm{L}}+P)-I_{xy}(Q_{\mathrm{L}}+Q)-I_{xz}(R_{\mathrm{L}}+R)\right](Q_{\mathrm{L}}+Q)\\
&+I_z\dot{R}-I_{zx}\dot{P}-I_{zy}\dot{Q}=N. \qquad (5)
\end{aligned}
$$

Non-linear part of response (Eq.5) is evaluated in the time domain yielding the velocities u,v,w,P,Q,R of the ship in the body-fixed co-ordinate system. Numerical integration is coducted using the Runge-Kutta routine of the 4rd order. At each time step, equations (5) are decoupled by solving a system of the linear algebraic equations. The non-linear portion is comprised of the cross-coupling terms of the body dynamics and the non-linear parts of the restoring and Froude-Krylov forces. Ship resistance and the action of rudder and propeller are taken into account as well. The ship hull is represented by a three-dimensional panel model when evaluating the restoring and the Froude-Krylov forces. Radiation and diffraction forces are assumed to be sufficiently well represented by the linear model. Radiation forces in time domain are obtained making use of the so-called retardation function formulation. Details of this approach are given in reference [6].

Velocities are integrated into the position of ship's centre of gravity (X_G,Y_G,Z_G) in the inertial co-ordinate system XYZ and into the Euler's angles ϕ,θ,ψ using the following transformations of the inertial and body-fixed co-ordinate systems [1, 2]:

$$
\begin{Bmatrix}\dot{X}_G\\ \dot{Y}_G\\ \dot{Z}_G\end{Bmatrix}=
\begin{bmatrix}
\cos\psi\cos\theta & \begin{matrix}\cos\psi\sin\theta\sin\phi\\ -\sin\psi\cos\phi\end{matrix} & \begin{matrix}\cos\psi\sin\theta\cos\phi\\ +\sin\psi\sin\phi\end{matrix}\\
\sin\psi\cos\theta & \begin{matrix}\sin\psi\sin\theta\sin\phi\\ +\cos\psi\cos\phi\end{matrix} & \begin{matrix}\sin\psi\sin\theta\cos\phi\\ -\cos\psi\sin\phi\end{matrix}\\
-\sin\theta & \cos\theta\sin\phi & \cos\theta\cos\phi
\end{bmatrix}
\begin{Bmatrix}u\\ v\\ w\end{Bmatrix}
$$

$$
\begin{Bmatrix}\dot{\phi}\\ \dot{\theta}\\ \dot{\psi}\end{Bmatrix}=
\begin{bmatrix}
1 & \sin\phi\tan\theta & \cos\phi\tan\theta\\
0 & \cos\phi & -\sin\phi\\
0 & \sin\phi/\cos\theta & \cos\phi/\cos\theta
\end{bmatrix}
\begin{Bmatrix}P\\ Q\\ R\end{Bmatrix}. \qquad (6)
$$

Both co-ordinate systems are presented in Figure 2.

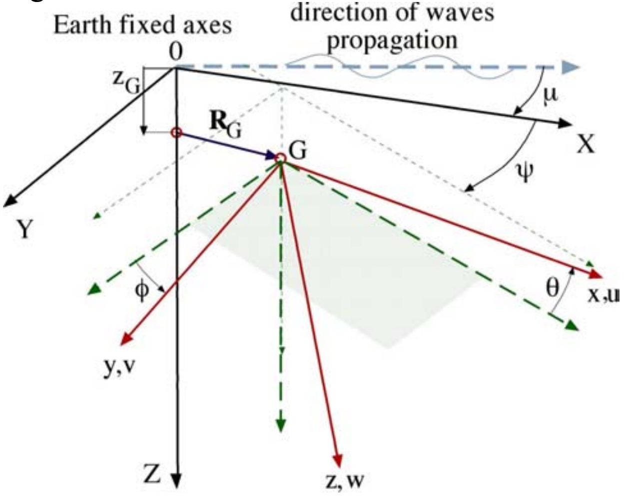

Fig. 2 Co-ordinate systems used to describe ship motion.

3 SIMULATION OF THE PARAMETRIC ROLL RESONACE

The simulated cases were selected so that the frequencies of encounter were twice the natural frequencies of roll. This was accomplished by small adjustments of the target KG-values with the ship target speed and wave length values kept constant. Model tests [4] were conducted

with the ship model equipped with the bilge keels of two size and without them. In the figures damping is given as the critical damping ratio ξ and natural period of roll is denoted as T_ϕ. These values were obtained in the tests and the same values were used in the simulations.
The effect of wave height on an amplitude of roll is clearly visible in Figs. 3 – 6.

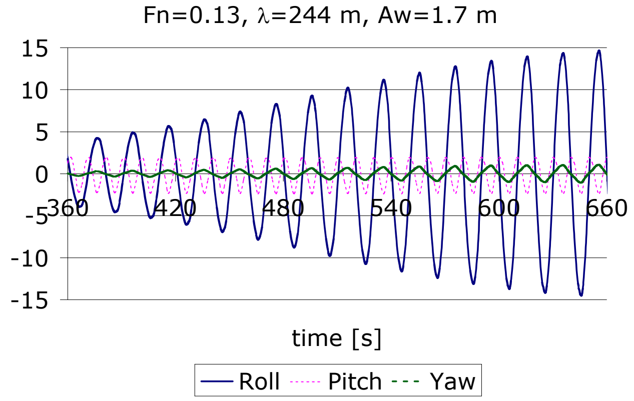

Fig. 3 Simulated angular motions for ship with low bilge keels and KG = 12 m. Wave amplitude A_W=1.7 [m]. T_ϕ = 20 [s], ξ = 0.046. Ultimate roll amplitude 16 [deg].

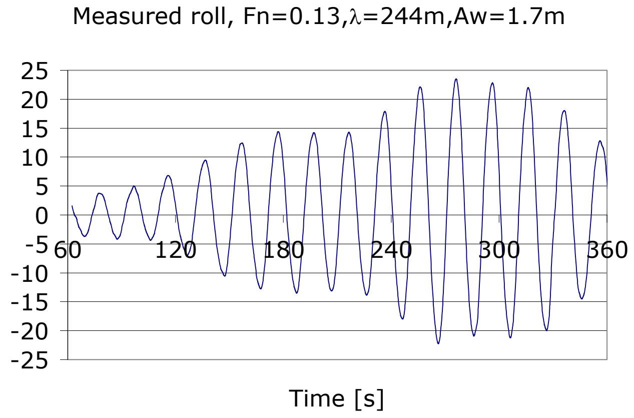

Fig. 4 Measured roll for ship equipped with low bilge keels and KG = 12 m. Wave amplitude A_W=1.7 [m]. T_ϕ = 20 [s], ξ = 0.046.

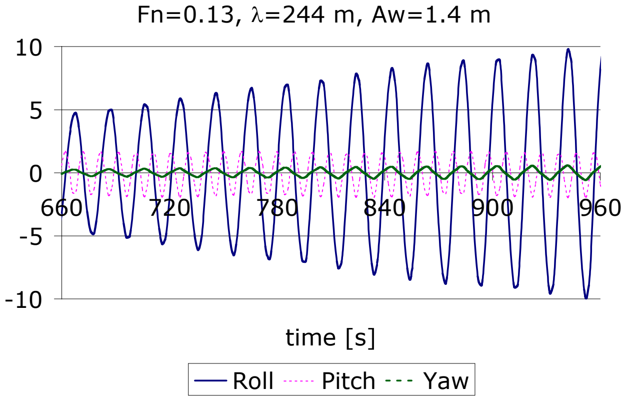

Fig. 5 Simulated angular motions for ship with low bilge keels and KG = 12 m. Wave amplitude A_W=1.4 [m]. T_ϕ = 20 [s], ξ = 0.046. Ultimate roll amplitude is 11 [deg].

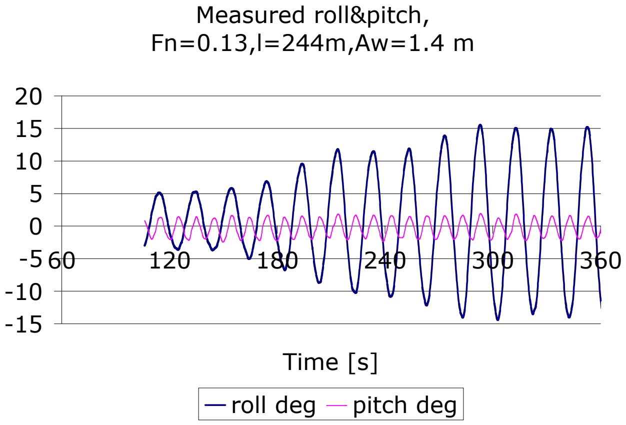

Fig. 6 Measured roll for ship equipped with low bilge keels and KG = 12 m. Wave amplitude A_W=1.4 [m]. T_ϕ = 20 [s], ξ = 0.046.

Both the simulations and the model test experiments give similar conclusion. In this case of a pure parametric resonance, where the ratio of an encounter period to roll natural period is 0.5, roll amplitude seems to be related to wave amplitude squared. Moreover, an increase of the wave amplitude results in a lower number of encounter periods required for a roll motion to start. Simulations indicate that there is a certain threshold value of wave amplitude below which paramatric roll resonance does not develop.

The effect of bilge keels height on the roll amplitude is readible from Figs. 7 – 10. Both the simulations and the tests indicate that an increase of damping results in a somewhat lower roll amplitude. It also delays and slowers the development of the parametric roll resonance. An increasing yaw motion is visible in Fig. 7, too. Pitch is not affected by the roll motion.

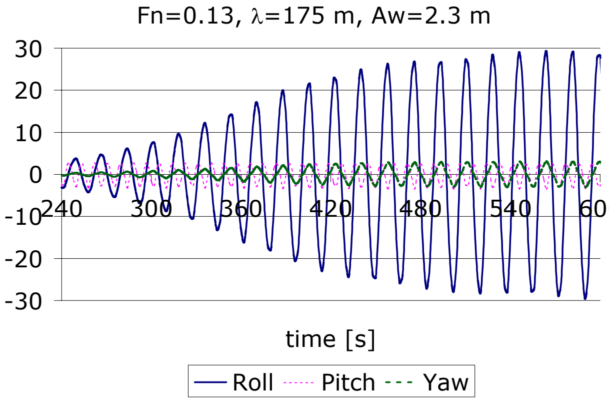

Fig. 7 Simulated angular motions for ship without bilge keels and KG = 11.5 m. Wave amplitude A_W=2.3 [m]. T_ϕ = 17.3 [s], ξ = 0.045.

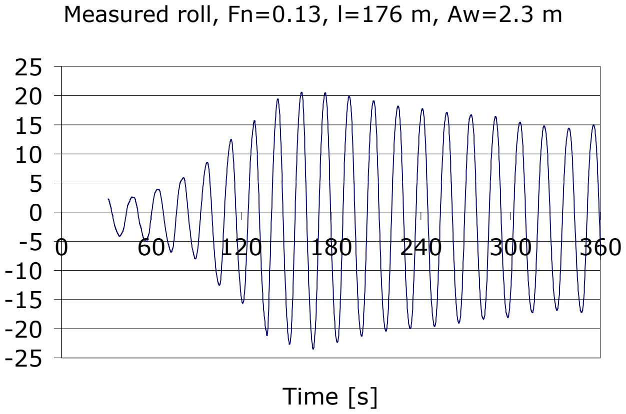

Fig. 8 Measured roll for ship without bilge keels and KG = 11.5 m. Wave amplitude A_W=2.3 [m]. T_ϕ = 17.3 [s], ξ = 0.045.

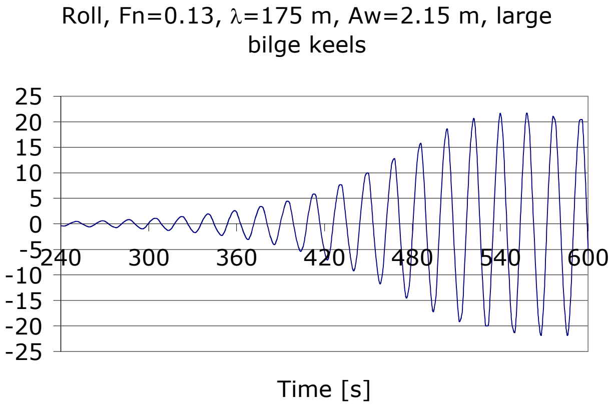

Fig. 9 Simulated roll for large bilge keels and KG = 11.5. Wave amplitude A_W =2.15 [m]. T_ϕ = 21.1 [s], ξ = 0.065.

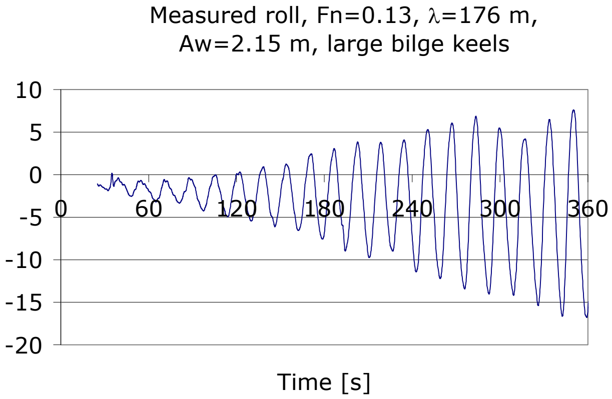

Fig. 10 Measured roll for large bilge keels and KG = 11.5. Wave amplitude A_W =2.15 [m]. T_ϕ = 21.1 [s], ξ = 0.065.

The absence of bilge keels results in a still higer roll amplitude and a faster development of roll motion (refer to Figs. 11 and 12).

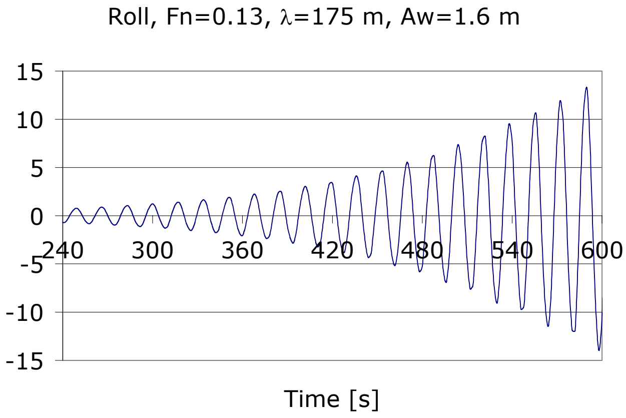

Fig. 11 Simulated roll for ship without bilge keels and KG = 11.5 m. Wave amplitude A_W=1.6 [m]. $T_\phi = 17.3$ [s], $\xi = 0.045$. Ultimate roll amplitude is 21 [deg].

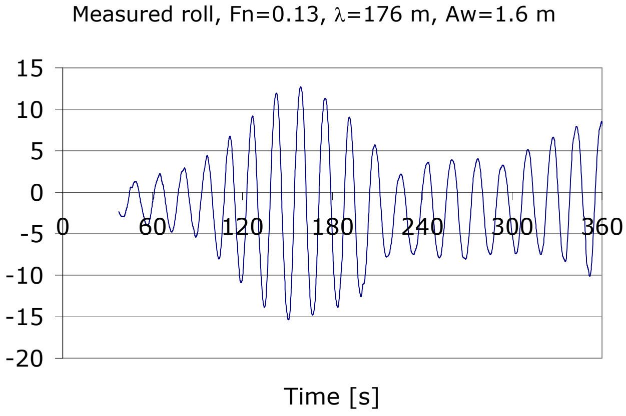

Fig. 12 Measured roll for ship without bilge keels and KG = 11.5 m. Wave amplitude A_W=1.6 [m]. $T_\phi = 17.3$ [s], $\xi = 0.045$.

The effect of the initial heel on the parametric roll resonance can be deduced using the result of simultion presented in Fig. 13 and comparing it with Fig. 7. The simulated case is the same as presented in Figs. 7 and 8. The initial value of heel of 2 [deg] is applied. Small initial heel decreases the number of the encounter periods required for the parametric roll to develop. The ultimate roll amplitude seems to be independent upon the small disturbances due to the non-zero initial conditions.

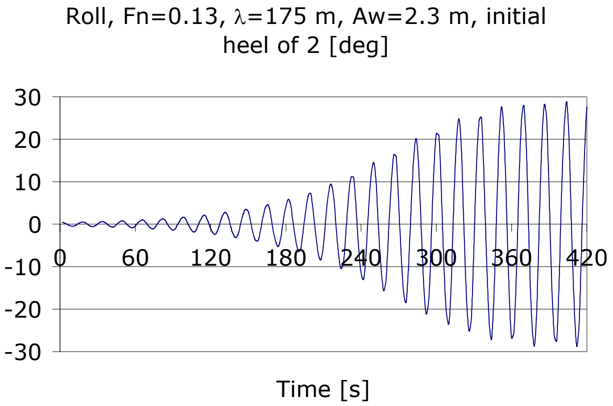

Fig. 13 Simulated angular motions for ship without bilge keels and KG = 11.5 m. Wave amplitude A_W=2.3 [m]. $T_\phi = 17.3$ [s], $\xi = 0.045$. Initial heel of 2 [deg].

4 CONCLUSIONS

Calculations conducted using the two-stage approach reveal parametric resonance of roll motion in head waves, which was observed in the model tests. The method can cope with the non-linearities associated with the parametric roll resonance. It also reveals roll-to-yaw coupling during this resonant motion.

The effect of wave amplitude and roll damping on the roll response is reproduced well by the numerical simulations. The initial conditions used in the calculations do not seem to have an effect on the developed resonant motion. They have an effect on the time required for the resonant motion to start.

5 REFERENCES

[1] Clayton B.R.& Bishop R.E.D 1982 Mechanics of marine vehicles, ISBN 0 419 12110-2.

[2] Fossen, T.,I. 1994 Guidance and control of ocean vehicles, J. Wiley&SonsISBN 0 471 94113 1.

[3] Journee. J. M. Strip Theory Algorithms, report MEMT 24, Delft University of Technology, Ship Hydrodynamics Laboratory. 1992.

[4] Mattila, M. An investigation of the dynamic stability of a fast RoPax vessel in waves (in Finnish), Helsinki University of Technology, Mechanical Engineering Department, Master Thesis, 1999.

[5] Matusiak, J. Two-Stage Approach To Determination Of Non-Linear Motions Of Ship In Waves, 4th Osaka Colloquium on Seakeeping Performance of Ships, Osaka, Japan, 17-21st October, 2000

[6] Matusiak, J. Importance Of Memory Effect For Capsizing Prediction, 5th International Workshop On Ship Stability, University of Trieste 12. - 13. September 2001.